Original Article

Deep learning reconstruction versus iterative reconstruction for cardiac CT angiography in a stroke imaging protocol: reduced radiation dose and improved image quality

Angélique Bernard[1], Pierre-Olivier Comby[1], Brivaël Lemogne[1], Karim Haioun[2], Frédéric Ricolfi[1], Olivier Chevallier[3], Romaric Loffroy[3]

[1]Department of Neuroradiology and Emergency Radiology, François-Mitterrand University Hospital, Dijon, France; [2]Computed Tomography Division, Canon Medical Systems France, Suresnes, France; [3]Department of Cardiovascular and Interventional Radiology, ImViA Laboratory-EA 7535, François-Mitterrand University Hospital, Dijon, France

Correspondence to: Prof. Romaric Loffroy, MD, PhD, FCIRSE. Department of Cardiovascular and Interventional Radiology, Image-Guided Therapy Center, ImViA Laboratory-EA 7535, François-Mitterrand University Hospital, 14 Rue Paul Gaffarel, BP 77908, 21079 Dijon Cedex, France. Email: romaric.loffroy@chu-dijon.fr.

Background: To assess the radiation dose and image quality of cardiac computed tomography angiography (CCTA) in an acute stroke imaging protocol using a deep learning reconstruction (DLR) method compared to a hybrid iterative reconstruction algorithm.

Methods: Retrospective analysis of 296 consecutive patients admitted to the emergency department for stroke suspicion. All patients underwent a stroke CT imaging protocol including a non-enhanced brain CT, a brain perfusion CT imaging if necessary, a CT angiography (CTA) of the supra-aortic vessels, a CCTA and a post-contrast brain CT. The CCTA was performed with a prospectively ECG-gated volume acquisition. Among all CT scans performed, 143 were reconstructed with an iterative reconstruction algorithm (AIDR 3D, adaptive iterative dose reduction three dimensional) and 146 with a DLR algorithm (AiCE, advanced intelligent clear-IQ engine). Image noise, signal-to-noise ratio (SNR), contrast-to-noise ratio (CNR), and subjective image quality (IQ) scored from 1 to 4 were assessed. Dose-length product (DLP), volume CT dose index (CTDIvol) and effective dose (ED) were obtained.

Results: The radiation dose was significantly lower with AiCE than with AIDR 3D (DLP =106.4±50.0 *vs.* 176.1±37.1 mGy·cm, CTDIvol =6.9±3.2 *vs.* 11.5±2.2 mGy, and ED =1.5±0.7 *vs.* 2.5±0.5 mSv) (P<0.001). The median SNR and CNR were higher [9.9 (IQR, 8.1–12.3); and 12.6 (IQR, 10.5–15.5), respectively], with AiCE than with AIDR 3D [6.5 (IQR, 5.2–8.5); and 8.4 (IQR, 6.7–11.0), respectively] (P<0.001). SNR and CNR were increased by 51% and 49%, respectively, with AiCE compared to AIDR 3D. The image quality was significantly better with AiCE (mean IQ score =3.4±0.7) than with AIDR 3D (mean IQ score =3±0.9) (P<0.001).

Conclusions: The use of a DLR algorithm for cardiac CTA in an acute stroke imaging protocol reduced the radiation dose by about 40% and improved the image quality by about 50% compared to an iterative reconstruction algorithm.

Keywords: Computed tomography angiography (CTA); cardiac imaging; artificial intelligence; image reconstruction; deep learning

Submitted Apr 30, 2020. Accepted for publication Aug 28, 2020.
doi: 10.21037/qims-20-626
View this article at: http://dx.doi.org/10.21037/qims-20-626

Introduction

According to the World Health Organization, 15 millions of people suffer from a stroke each year worldwide (1). The mortality rate is steadily declining as a result of therapeutic progress, but strokes often remain responsible for severe neurological sequelae and represent a real public health issue (2). Imaging plays a central role in the care chain to diagnose stroke. Computed tomography (CT) is recommended as the initial modality of choice for stroke investigation thanks to its accessibility and rapidity (3). The recurrence rate of events in the first year after an acute stroke is estimated to be 7% to 13 % (4). Therefore, the cause of initial ischemic stroke needs to be investigated to treat and prevent a second stroke.

Cardioembolic etiology is responsible for 20% to 30% of ischemic strokes, especially atrial fibrillation and thrombus in the left atrial appendage (LAA) (5). Trans-esophageal echocardiography (TEE) is the gold standard to detect LAA thrombi (6). However, TEE is not routinely performed during the hospitalization, is time-consuming and semi-invasive which is restrictive or even contraindicated in patients with acute stroke (7). In our institution, we now systematically perform a cardiac CT angiography (CCTA) in all patients with stroke symptoms as part of their initial stroke work-up to determine if there is a cardioembolic cause to the stroke.

Because of the increased number of CTs performed every year in such a setting, every effort has been made to reduce radiation dose as much as possible using iterative reconstruction (8). One of the existing technologies used to decrease radiation dose to the patient without changing clinical workflow is called Adaptive Iterative Dose Reduction 3D (AIDR 3D) (9). More recently, with the emergence of artificial intelligence, a deep learning based reconstruction (DLR) technique has been developed for CT [Advanced Intelligent Clear-IQ Engine (AiCE)] (10,11). The algorithm uses a deep convolutional neural network (DCNN) to identify true signal from noise in the image. Thus, DLR can remove noise from the signal, creating high quality images with reduced radiation dose.

The aim of the present study was to evaluate the image quality and the radiation dose of DLR technology compared to an iterative reconstruction for cardiac CTA performed as part of a stroke imaging protocol.

Methods

Patients

From November 2018 to February 2019, 296 consecutive patients with suspected acute stroke were enrolled in this retrospective study. From November 1st, 2018 to December 13th, 2018, 148 patients with stroke symptoms were scanned with iterative reconstruction (AIDR 3D). On December 14th, 2018, DLR was installed on our CT machine. Then, 148 patients with acute stroke symptoms were scanned with DLR until February 4th, 2019. All patients were referred from the emergency department or other departments at our tertiary University Hospital. Standard exclusion criteria for contrast-enhanced CT were applied including allergy to iodinated contrast, renal disease, and pregnancy. Patients with missing data, especially acquisition data or with a ventricular support system were also excluded. According to institutional policy, approval from our Institutional Review Board was not required.

DLR

The network is formed by a complex of neurons that performs similar to the human brain (11). The DCNN is trained using thousands of pairs of data, one low quality (noisy) and one high quality (low noise). The network learns to create the high-quality results from the low-quality data by comparing the results with the gold standard high-quality data reconstructed with advanced Model-Based Iterative Reconstruction (MBIR). Once the training is completed, the DCNN is validated using new data before being locked for use in clinical practice where it does not continue to learn. DLR process is trained to differentiate noise and signal in images and improve signal while suppressing noise to obtain high-quality images. AiCE is also fully integrated into the automatic exposure control system. The system automatically adjusts each individual patient's mA profile based on the associated benefits and dose reduction abilities of AiCE reconstruction.

CT examination

CT scans were performed using an Aquilion ONE GENESIS machine (Canon Medical Systems, Otawara, Japan). As patients were scanned in an emergency setting, the arms were placed down by the side. The scan range was determined from the scanogram to include the heart with a maximum length of 16 cm (*Figure 1*). Our stroke imaging protocol consisted of the 5 following steps: a non-enhanced brain CT, a brain perfusion CT if necessary, a cranio-caudal supra-aortic vessels CTA, then a CCTA, and finally a post-contrast brain CT.

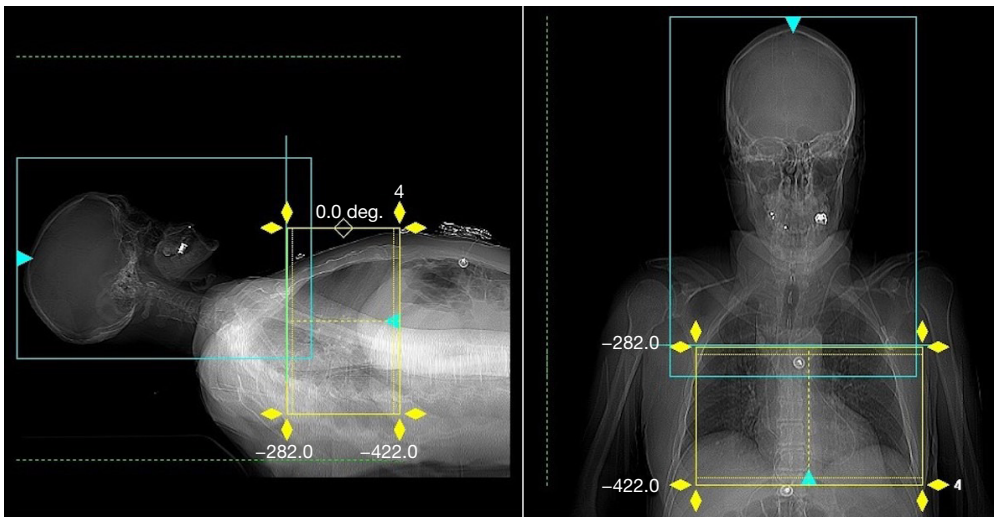

Figure 1 Scan plan protocol for the carotid (blue box) and the cardiac (yellow box) computed tomography acquisition.

If patients were eligible for thrombolytic therapy, a brain perfusion CT was performed. A bolus of 40 mL of nonionic contrast agent (Iomeron 350, Bracco Imaging, Italy) was injected at a rate of 5 mL/s followed by 40 mL of saline at the same rate via an 18 G needle from the right or left arm. For the carotid and CCTA, a three-phase protocol was used: injection of 50 mL of nonionic contrast agent at a rate of 5 mL/s followed by 60 mL of a contrast/saline mixture (50% contrast and 50% saline) at a flow rate of 3.5 mL/s, followed by 50 mL of saline at a rate of 3.5 mL/s. Bolus tracking software (^{SURE}Start, Canon Medical) was used to initiate the carotid scan immediately followed by the cardiac scan. A region of interest (ROI) was placed in the aorta arch and the scan was triggered when the Hounsfield units (HU) value within the ROI reached 150–170 HU.

A prospective ECG-gated volume scan was performed during a single heartbeat. The target scan phase was calculated automatically by the CT scanner based on the patient's heart rate (^{SURE}Cardio, Canon Medical). Images were reconstructed at the most motion-free cardiac phase as determinated automatically by the CT scanner (PhaseXact, Canon Medical) at either the end diastolic or systolic phase of RR cycle. Beta blockers were not administered as the patients were emergent and the intent of the CCTA was to investigate the LAA rather than the coronary arteries. A single breath hold command was given for the carotid CT and cardiac CT if the patient was able to understand. Immediately following the carotid scan, the cardiac CT was performed with the same contrast injection. The mean time of cardiac CT after injection was 36.1±4.5s. The scan parameters for the cardiac CT were as follows: tube voltage 120 kVp, automatic tube current modulation (^{SURE}Exposure 3D) 40–650 mA, collimation 320 mm × 0.5 mm, field of view 230 mm, rotation time 0.275 s (*Table 1*).

Image acquisition and reconstruction

Cardiac images were reconstructed with a slice thickness of 0.5 mm and an increment of 0.25 mm. Adaptive Iterative Dose Reduction using three Dimensional (AIDR 3D, Canon Medical, Otawara, Japan) was used for the first 148 patients, then DLR with Advanced Intelligent Clear-IQ Engine (AiCE, Canon Medical, Otawara, Japan) for the remaining 148 patients. DLR was only applied for cardiac CT images because not yet available from the Canon constructor for the other scan components of the stroke imaging protocol in the first and early version used in the present study.

Image quality, signal-to-noise and contrast-to-noise evaluation

All images were analyzed using a workstation (Centricity Universal Viewer, GE Healthcare, General Electric Company, United States, version 6.0). Measurements were performed by one radiologist with 4 years of experience. A circular ROI with a fixed area of 1.0±0.2 cm^2 was placed in the center of the ascending aorta, in fat within the mediastinum, in the left atrium and in the myocardium within the lateral wall of the left ventricle. Signal was defined as the mean CT value in HU and noise was defined as the standard

Table 1 Acquisition parameters for the cardiac computed tomography

Parameters	Outcomes
Tube voltage (kVp)	120
Tube current ± SD (mA)	Automatic tube current modulation (^{SURE}Exposure 3D) [40–650]±40
Collimation (mm)	320×0.5
Rotation time (s)	0.275
Field of view (mm)	230
Exposure window (ms)	300
Slice thickness (mm)	0.5
Interval (mm)	0.25
Pitch	Not applicable

kVp, kilovoltage peak; mA, milliampere; SD, standard deviation; mm, millimeter; s, second; ms, millisecond.

deviation (SD) within the ROI. Image noise was defined as the standard deviation of the CT value in the mediastinal fat or left ventricular myocardium (12,13). Signal-to noise ratio (SNR) and contrast-to-noise ratio (CNR) were then defined according to the following formula:

SNR aorta = signal CT aorta/SD and CNR aorta = (signal CT aorta – signal CT fat)/SD

Subjective image quality (IQ) was also assessed. IQ was visually scored according to a four-point scale by two radiologists with 4 and 7 years of experience who were blinded to the reconstruction method and CT parameters: 1= poor (non-diagnostic), 2= suboptimal (some artifacts with possible diagnosis), 3= good (few artifacts that do not interfere with sufficient diagnosis), 4= excellent (no artifact, well-diagnostic) (14). Disagreement was resolved by consensus.

Radiation dose assessment

Volume CT dose index ($CTDI_{vol}$) and dose-length product (DLP) were used to obtain the radiation dose. Effective dose (ED) was calculated by multiplying the DLP with the International Commission on Radiological Protection conversion factor for cardiac CT imaging (0.014 mSv/mGy·cm) (15,16).

Statistical analysis

Continuous variables were presented as means ±SD for Gaussian distribution, and as medians (first quartile–third quartile) for non-Gaussian distribution after the Kolmogorov-Smirnov test. Dichotomous variables were presented as numbers (percentages). For categorical data, a Chi-square or Fischer exact test was used, while a Student's *t*-test was used for the comparison of continuous data with normal distribution variables or a Mann-Whitney test for non-parametric variables. The threshold of significance was set at 5% (P<0.05). All statistical tests were performed using the STATA® software (version 13; StataCorp) and Excel Software (version 2016).

Results

Patient population

From November 2018 to February 2019, 296 patients were admitted for acute stroke-like symptoms. Overall, 289 were included in the study for analysis: 143 patients in the AIDR 3D group and 146 patients in the AiCE group. Seven patients were excluded: 6 because of missing data and 1 because of the presence of a ventricular support system (Impella®). The clinical characteristics of the patients and the flow chart of the study are summarized in *Table 2* and *Figure 2*, respectively. There was no significant difference between the 2 groups for age, gender, weight, body mass index (BMI) or heart rate (P>0.05).

Image quality

There was no significant difference in the reconstruction phase of the heart cycle between AIDR 3D and AiCE groups, neither in the end diastolic phase (75% of the RR) nor systolic phase (40% of the RR) (P=0.319) (*Table 3*).

The analysis of image quality evaluation is summarized in *Table 4*. The SNR ascending aorta (AA), SNR left atrium (LA), CNR AA and CNR LA with AiCE were significantly higher than with AIDR 3D (P<0.001). For the ascending aorta, the median SNR and CNR were 9.9 and 12.6, respectively, with AiCE, whereas the median SNR and CNR were 6.5 and 8.4, respectively, with AIDR 3D (P<0.001). There was an increase of 51% of the SNR AA and of 49% of the CNR AA with AiCE compared to AIDR 3D. There was an increase of 60% of the SNR LA and of 73% of the CNR LA with AiCE compared to AIDR 3D.

The subjective image quality was also significantly better with AiCE than with AIDR 3D. Indeed, the mean IQ score was 3.4±0.7 with AiCE versus 3±0.9 with AIDR 3D (P<0.001). *Figures 3* and *4* illustrate the differences between

Table 2 Characteristics of the study population.

Characteristics	AIDR 3D (n=143)	AiCE (n=146)	P value
Age (years)	72 [58–82]	73 [61–84]	0.724
Male gender	77 (53.8%)	69 (47.3%)	0.264
Weight (kg)	69.9±16	71.4±16.4	0.499
BMI (kg/m²)	25.4±5.1	25.8±5.2	0.603
Heart rate (bpm)	77.7±18.2	81.8±19.2	0.103

Data are presented as mean ± standard deviation, median (interquartile range) or number (percentage). P values <0.05 were considered significant. AIDR 3D, adaptive iterative dose reduction three dimensional; AiCE, advanced intelligent clear-IQ engine; n, number; kg, kilogrammes; BMI, body mass index; bpm, beats per minute.

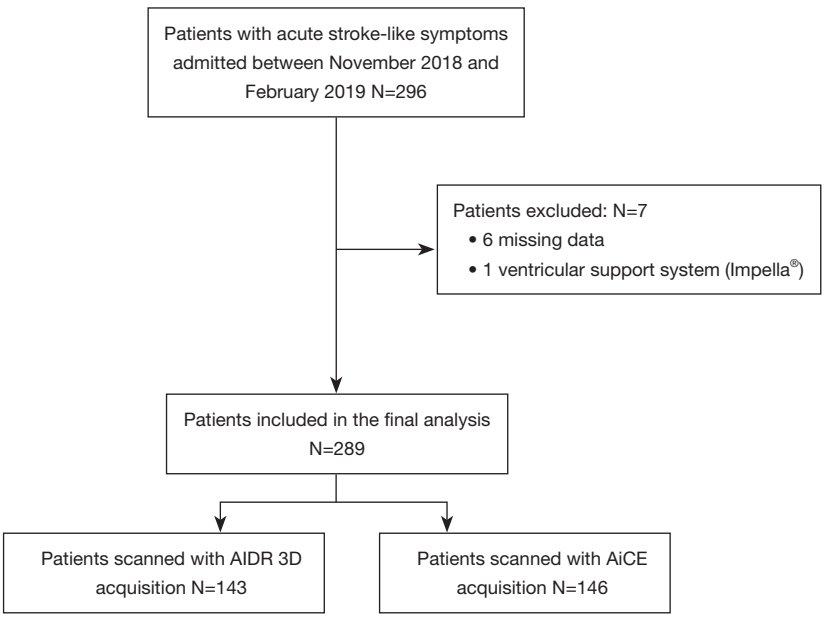

Figure 2 Flow chart of the population study.

Table 3 Computed tomography reconstruction based on heart rate: end diastolic phase (75% of the RR) or systolic phase (40% of the RR)

Variable	AIDR 3D (n=143)	AiCE (n=146)	P value
75% of RR	74 (51.7%)	67 (45.9%)	0.319
40% of RR	69 (48.3%)	79 (54.1%)	0.319

Data are presented as number (percentage). P values <0.05 were considered significant. AIDR 3D, adaptive iterative dose reduction three dimensional; AiCE, advanced intelligent clear-IQ engine; n, number.

the two methods of reconstruction.

Radiation dose

Comparison results of radiation dose between AIDR 3D and AiCE are summarized in *Table 5* and *Figure 5*. The mean DLP was significantly lower with AiCE (106.4± 50.0 mGy·cm) than with AIDR 3D (176.1±37.1 mGy·cm) (P<0.001). The mean $CTDI_{vol}$ was significantly lower with AiCE (6.9±3.2 mGy) than with AIDR 3D (11.5±2.2 mGy)

Table 4 Signal-to-noise ratio (SNR) and contrast-to-noise ratio (CNR) analysis

Variable	AIDR 3D (n=143)	AiCE (n=146)	P value
SNR AA	6.5 (5.2–8.5)	9.9 (8.1–12.3)	<0.001
CNR AA	8.4 (6.7–11.0)	12.6 (10.5–15.5)	<0.001
SNR LA	5.9 (4.5–7.5)	9.1 (7.5–11.2)	<0.001
CNR LA	3.0 (2.0–3.9)	4.8 (3.7–6.3)	<0.001

Data are presented as median (interquartile range). P values <0.05 were considered significant. AIDR 3D, adaptive iterative dose reduction three dimensional; AiCE, advanced intelligent clear-IQ engine; n, number; AA, ascending aorta; LA, left atrium.

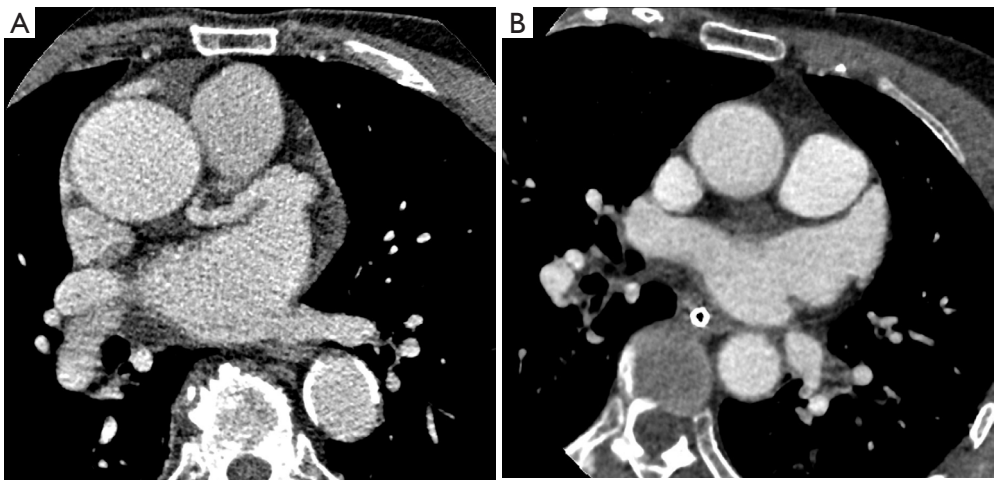

Figure 3 Examples of cardiac computed tomography scans in two patients with same weight of 60 kg. (A) AIDR 3D with a DLP of 202.1 mGy·cm and $CTDI_{vol}$ of 12.6 mGy, and (B) AiCE with a DLP of 23.3 mGy·cm and $CTDI_{vol}$ of 1.7 mGy. AIDR 3D, adaptive iterative dose reduction three dimensional; DLP, dose-length product; AiCE, advanced intelligent clear-IQ engine.

(P<0.001). Last, the mean ED was significantly lower with AiCE (1.5±0.7 mSv) than with AIDR 3D (2.5±0.5 mSv) (P<0.001).

Regarding the overall dose reduction for the complete comprehensive stroke imaging protocol, excluding supra-aortic CTA, results were as follows: the mean DLP with AIDR 3D (1,181.5±266.6 mGy·cm without brain CT perfusion and 2,940.0±296.1 mGy·cm with brain CT perfusion, respectively) did not differ significantly from that with AiCE (1,219.0±885.7 mGy·cm without brain CT perfusion and 2,921.0±845.9 mGy·cm with brain CT perfusion, respectively) (P>0.05). Similarly, the mean $CTDI_{vol}$ with AIDR 3D (66.9±3.9 mGy without brain CT perfusion and 154.6±38.2 mGy with brain CT perfusion, respectively) did not differ significantly from that with AiCE (67.1±3.5 mGy without brain CT perfusion and 151.0±37.7 mGy with brain CT perfusion, respectively) (P>0.05).

Overall, the mean DLP and $CTDI_{vol}$ including cardiac CT and supra-aortic CTA scans were significantly lower with AiCE (293.3±83.5 mGy·cm and 10.9±13.9 mGy, respectively) than with AIDR 3D (404.5±266.6 mGy·cm and 16.1±15.0 mGy, respectively) (P<0.001), for an overall dose reduction for the complete comprehensive stroke imaging protocol of 28%, due to AI applied for cardiac CT imaging.

Discussion

This study was designed to retrospectively compare DLR with iterative reconstruction in the assessment of image quality and radiation dose of CCTA in a stroke imaging protocol. The results indicated that DLR allowed both a significant improvement of the image quality and a significant reduction of radiation dose. The study demonstrated both an improvement of SNR and CNR by approximately 51% and 49%, respectively. Our results showed that the most important part of overall radiation

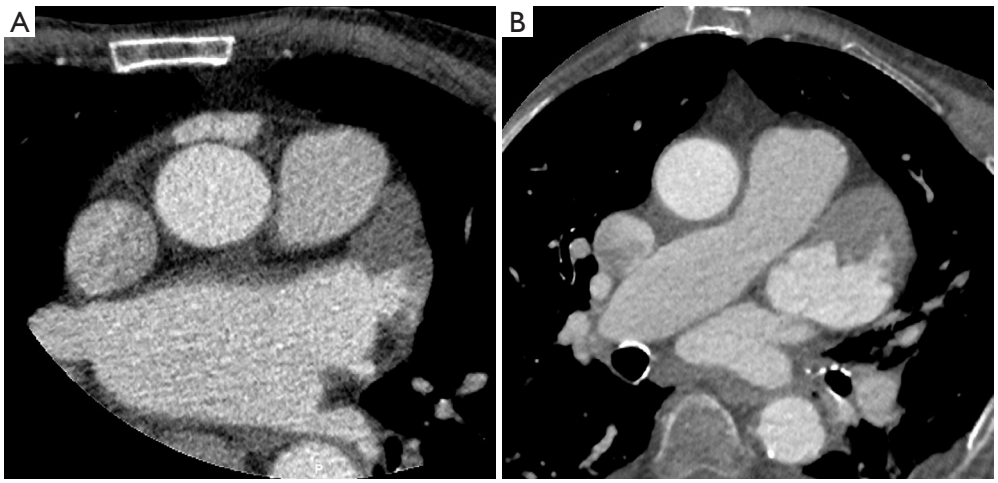

Figure 4 Left atrial appendage thrombus on cardiac computed tomography in two patients with same weight of 60 kg. (A) AIDR 3D with a DLP of 177.3 mGy·cm and $CTDI_{vol}$ of 11.1 mGy, and (B) AiCE with a DLP of 42.1 mGy·cm and $CTDI_{vol}$ of 2.6 mGy. AIDR 3D, adaptive iterative dose reduction three dimensional; DLP, dose-length product; AiCE, advanced intelligent clear-IQ engine.

Table 5 Comparison of radiation dose between AIDR 3D and AiCE

Variable	AIDR 3D (n=143)	AiCE (n=146)	P value
DLP (mGy·cm)	176.1±37.1, 181.5 (166.4–204.2)	106.4±50.0, 104.4 (61.5–153.9)	<0.001
$CTDI_{vol}$ (mGy)	11.5±2.2, 12.7 (11.1–12.8)	6.9±3.2, 6.6 (3.9–10.0)	<0.001
ED (mSV)	2.5±0.5, 2.5 (2.3–2.9)	1.5±0.7, 1.5 (0.9–2.2)	<0.001

Data are presented as mean ± standard deviation and median (interquartile range). P values <0.05 were considered significant. AIDR 3D, adaptive iterative dose reduction three dimensional; AiCE, advanced intelligent clear-IQ engine; n, number; DLP, dose-length product; $CTDI_{vol}$, volume computed tomography dose index; ED, effective dose.

dose was related to the "other than cardiac" CT imaging components, especially brain CT perfusion, as expected. No significant difference was found between techniques in terms of radiation for all other scan components than cardiac CT imaging since AI was not available for these components. The difference in radiation dose was due to AI applied for cardiac CT imaging.

Some recent studies showed higher image quality of coronary CT with DLR versus hybrid iterative reconstruction, and higher image quality of abdominal ultra-high resolution CT with DLR versus Model-Based Iterative Reconstruction (17,18). The strength of the present study was that our sample of 289 patients was larger than prior studies using DLR. To our knowledge, this is the largest comparative study to date evaluating DLR versus iterative reconstruction algorithm for CCTA.

Moreover, this study included DLR in the automatic exposure control settings, allowing us to evaluate the radiation dose reduction. We demonstrated that DLR allowed a reduction of radiation dose by about 40% for cardiac CTA as part of a stroke imaging protocol compared to the use of an iterative reconstruction. Geyer *et al.* underlined the importance of reducing radiation dose levels without decreasing the image quality (19).

Many studies demonstrated that decreasing the radiation dose may lead to reduced image quality and increased noise. Thus, DLR is able to reduce radiation dose while increasing the image quality. The phantom study of Gervaise *et al.* showed a significant reduction of image noise with an equivalent dose comparing AIDR 3D to the traditional Filtered Back Projection reconstruction (20). Other investigators shown that radiation dose can be reduced when using AIDR 3D (9,21,22).

It is important to underline the need for reducing the radiation dose. Indeed, with the increasing number of CT exams performed widely, the dose delivered to the patient has

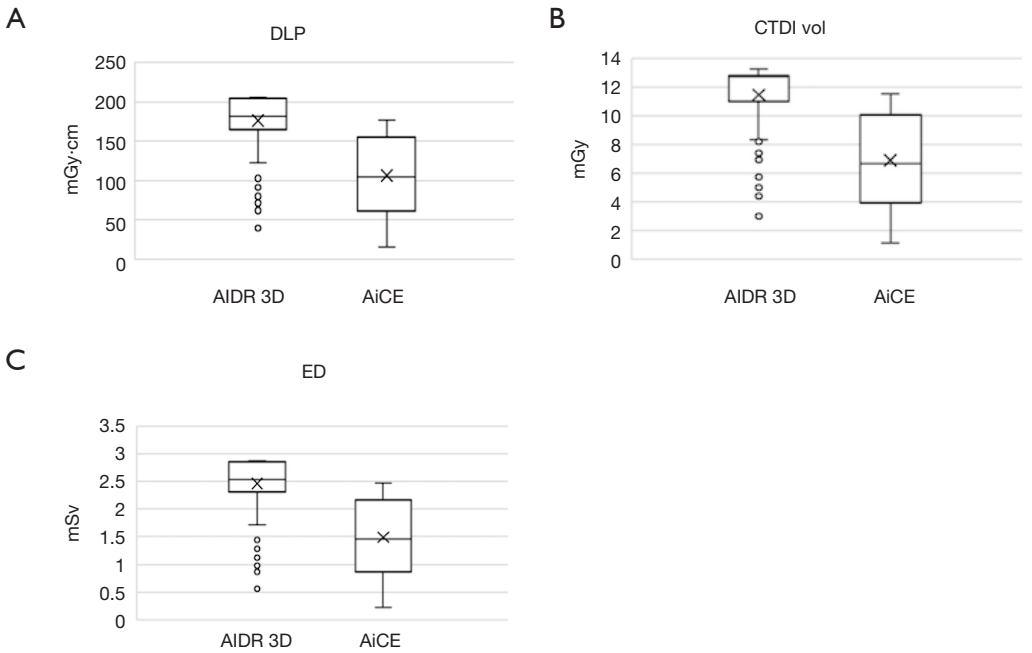

Figure 5 Box-plots comparing AIDR 3D and AiCE algorithms. (A) Dose-length product (DLP) (mGy·cm), (B) volume computed tomography dose index ($CTDI_{vol}$) (mGy), (C) effective dose (ED) (mSv). AIDR 3D, adaptive iterative dose reduction three dimensional; AiCE, advanced intelligent clear-IQ engine.

the potential risk of radiation-induced cancer, especially with cardiac acquisition which includes particularly radio-sensitive organs such as breasts, myocardium and coronaries (15). The lowest DLP with AiCE in our study was 16 mGy·cm, corresponding to an ED of 0.22 mSv, and the mean radiation dose with AiCE was 106 mGy·cm, corresponding to an average ED of 1.49 mSv. We also used a prospective acquisition technique which allowed a radiation dose reduction of about 70–80% compared to a retrospective cardiac CT acquisition method (23). Furthermore, the volume acquisition also helped to reduce the radiation dose.

However, higher radiation doses were expected because, in this emergency stroke imaging protocol, the arms were placed beside the body in order to minimize artifacts for the carotid CTA. Usually, in cardiac CTA examinations, the arms are placed above the patient head, out of the field of view, in order to reduce noise resulting from the increased soft tissue attenuation and to reduce radiation dose (24). Despite the arms position, there were few artifacts CCTA scans interfering with the interpretation. Indeed, the subjective image quality score was over 3 points on our scale, whatever the reconstruction algorithm used, which permitted normal diagnosis. Furthermore, an ECG-gated and very short acquisition (0.275 s) allowed the image quality to be less influenced by cardiac motion. The ED was 1.5 mSv with AiCE, which was lower than with AIDR 3D technique (9). Thanks to the low radiation dose permitted with DLR, the use of CCTA may be considered more frequently in emergent situations such as part of acute stroke imaging work-up or as an alternative to TEE when not available or impossible.

Our study had some limitations. First, the retrospective nature of the study was one of them. Second, images were acquired either at the end systolic or diastolic phase which can lead to differences in the image quality analysis due to motion artifacts. However, there was no significant difference in reconstruction phase of the heart cycle between the 2 groups, neither in the end systolic nor in the diastolic phase. Third, the study compared AIDR 3D and AiCE in different patients. Indeed, 2 cardiac CT scans could not be performed in the same patient because of multiple injections, radiation dose concerns and emergency setting. As AiCE is integrated into the mA modulation system, we performed CT scans with 2 reconstructions in different patients in order to compare radiation doses. However, all patients were scanned on the same CT machine and DLR was the only technical difference between the two groups. Last, DLR was only applied for cardiac CT images because

not yet available from the Canon constructor for the other scan components of the stroke imaging protocol in the first and early version used in the present study. The second version allowing to apply DLR for other scan components of the stroke imaging protocol, especially CT perfusion, should be available soon forward European premiere in our institution for further evaluation. In the meantime, the goal of the present study was to show that adding cardiac CT to the stroke imaging protocol is possible while reducing overall radiation dose and improving image quality.

Conclusions

In conclusion, the present study showed that the use of a DLR for CCTA in an acute stroke imaging protocol improved the image quality and reduced the radiation dose compared to the use of an iterative reconstruction. Therefore, these results demonstrate that a DLR technique may be clinically useful to improve diagnosis and patient care.

Acknowledgments

Funding: None.

Footnote

Conflicts of Interest: All authors have completed the ICMJE uniform disclosure form (available at http://dx.doi.org/10.21037/qims-20-626). KH works as a CT Clinical Research Scientist for Canon Medical Systems Europe. RL serves as an unpaid Deputy Editor for *Quantitative Imaging in Medicine and Surgery*. The other authors have no conflicts of interest to declare.

Ethical Statement: According to institutional policy of Dijon University, approval from our Institutional Review Board was not required owing the retrospective nature of the study. Written informed consent from the patient for publication of this study and any accompanying images was waived.

References

1. WHO EMRO | Stroke, Cerebrovascular accident | Health topics [Internet]. [cited 2019]. Available online: http://www.emro.who.int/health-topics/stroke-cerebrovascular-accident/index.html
2. Lackland DT, Roccella EJ, Deutsch AF, Fornage M, George MG, Howard G, Kissela BM, Kittner SJ, Lichtman JH, Lisabeth LD, Schwamm LH, Smith EE, Towfighi A; American Heart Association Stroke Council; Council on Cardiovascular and Stroke Nursing; Council on Quality of Care and Outcomes Research; Council on Functional Genomics and Translational Biology. Factors influencing the decline in stroke mortality: a statement from the American Heart Association/American Stroke Association. Stroke 2014;45:315-53.
3. Latchaw RE, Alberts MJ, Lev MH, Connors JJ, Harbaugh RE, Higashida RT, Hobson R, Kidwell CS, Koroshetz WJ, Mathews V, Villablanca P, Warach S, Walters B; American Heart Association Council on Cardiovascular Radiology and Intervention, Stroke Council, and the Interdisciplinary Council on Peripheral Vascular Disease. Recommendations for imaging of acute ischemic stroke: a scientific statement from the American Heart Association. Stroke 2009;40:3646-78.
4. Béjot Y, Bailly H, Durier J, Giroud M. Epidemiology of stroke in Europe and trends for the 21st century. Presse Med 2016;45:e391-8.
5. Yang H, Nassif M, Khairy P, de Groot JR, Roos YBBWEM, de Winter RJ, Mulder BJM, Bouma BJ. Cardiac diagnostic work-up of ischaemic stroke. Eur Heart J 2018;39:1851-60.
6. Vira T, Pechlivanoglou P, Connelly K, Wijeysundera HC, Roifman I. Cardiac computed tomography and magnetic resonance imaging vs. transoesophageal echocardiography for diagnosing left atrial appendage thrombi. Europace 2019;21:e1-10.
7. Popkirov S, Schlegel U, Weber W, Kleffner I, Altenbernd J. Cardiac imaging within emergency CT angiography for acute stroke can detect atrial clots. Front Neurol 2019;10:349.
8. Nelson RC, Feuerlein S, Boll DT. New iterative reconstruction techniques for cardiovascular computed tomography: how do they work, and what are the advantages and disadvantages? J Cardiovasc Comput

Tomogr 2011;5:286-92.
9. Chen MY, Steigner ML, Leung SW, Kumamaru KK, Schultz K, Mather RT, Arai AE, Rybicki FJ. Simulated 50% radiation dose reduction in coronary CT angiography using adaptive iterative dose reduction in three-dimensions (AIDR 3D). Int J Cardiovasc Imaging 2013;29:1167-75.
10. Dreyer KJ, Geis JR. When machines think: Radiology's next frontier. Radiology 2017;285:713-8.
11. Chen H, Zhang Y, Zhang W, liao P, Li K, Zhou J, Wang G. Low-dose CT via convolutional neural network. Biomed Opt Express 2017;8:679-94.
12. Muenzel D, Noel PB, Dorn F, Dobritz M, Rummeny EJ, Huber A. Coronary CT angiography in step-and-shoot technique with 256-slice CT: Impact of the field of view on image quality, craniocaudal coverage, and radiation exposure. Eur J Radiol 2012;81:1562-8.
13. Sabarudin A, Sun Z, Yusof AKM. Coronary CT angiography with single-source and dual-source CT: Comparison of image quality and radiation dose between prospective ECG-triggered and retrospective ECG-gated protocols. Int J Cardiol 2013;168:746-53.
14. Pahn G, Skornitzke S, Schlemmer HP, Kauczor HU, Stiller W. Toward standardized quantitative image quality (IQ) assessment in computed tomography (CT): A comprehensive framework for automated and comparative IQ analysis based on ICRU Report 87. Phys Med 2016;32:104-15.
15. Trattner S, Halliburton S, Thompson CM, Xu Y, Chelliah A, Jambawalikar SR, Peng B, Peters MR, Jacobs JE, Ghesani M, Jang JJ, Al-Khalidi H, Einstein AJ. Cardiac-specific conversion factors to estimate radiation effective dose from dose-length product in computed tomography. JACC Cardiovasc Imaging 2018;11:64-74.
16. Huda W, Magill D, He W. CT effective dose per dose length product using ICRP 103 weighting factors. Med Phys 2011;38:1261-5.
17. Tatsugami F, Higaki T, Nakamura Y, Yu Z, Zhou J, Lu Y, Fujioka C, Kitagawa T, Kihara Y, Iida M, Awai K. Deep learning-based image restoration algorithm for coronary CT angiography. Eur Radiol 2019;29:5322-9.
18. Akagi M, Nakamura Y, Higaki T, Narita K, Honda Y, Zhou J, Yu Z, Akino N, Awai K. Deep learning reconstruction improves image quality of abdominal ultra-high-resolution CT. Eur Radiol 2019;29:6163-71.
19. Geyer LL, Schoepf UJ, Meinel FG, Nance JW Jr, Bastarrika G, Leipsic JA, Paul NS, Rengo M, Laghi A, De Cecco CN. State of the art: Iterative CT reconstruction techniques. Radiology 2015;276:339-57.
20. Gervaise A, Osemont B, Lecocq S, Noel A, Micard E, Felblinger J, Blum A. CT image quality improvement using adaptive iterative dose reduction with wide-volume acquisition on 320-detector CT. Eur Radiol 2012;22:295-301.
21. Maeda E, Tomizawa N, Kanno S, Yasaka K, Kubo T, Ino K, Torigoe R, Ohtomo K. The feasibility of Forward-projected model-based Iterative Reconstruction SoluTion (FIRST) for coronary 320-row computed tomography angiography: A pilot study. J Cardiovasc Comput Tomogr 2017;11:40-5.
22. Zhao P, Hou Y, Liu Q, Ma Y, Guo Q. Radiation dose reduction in cardiovascular CT angiography with iterative reconstruction (AIDR 3D) in a swine model: a model of paediatric cardiac imaging. Clin Radiol 2016;71:716.e7-716.e14.
23. Earls JP, Berman EL, Urban BA, Curry CA, Lane JL, Jennings RS, McCulloch CC, Hsieh J, Londt JH. Prospectively gated transverse coronary CT angiography versus retrospectively gated helical technique: Improved image quality and reduced radiation dose. Radiology 2008;246:742-53.
24. Cardiac CT angiography: Patient-centric low-dose imaging [Internet]. [cited 2019]. Available online: https://appliedradiology.com/articles/cardiac-ct-angiography-patient-centric-low-dose-imaging

Cite this article as: Bernard A, Comby PO, Lemogne B, Haioun K, Ricolfi F, Chevallier O, Loffroy R. Deep learning reconstruction versus iterative reconstruction for cardiac CT angiography in a stroke imaging protocol: reduced radiation dose and improved image quality. Quant Imaging Med Surg 2021;11(1):392-401. doi: 10.21037/qims-20-626

